October 8, 1991 Presentation

Nowcasting Cloud Precipitation Fields Using the Remote Atmospheric Processing and Information Display (RAPID) System

PE 62101F
PR 6670
TA 10
WU 29

Frank H. Ruggiero, Kenneth F. Heideman

Phillips Lab/GAP
Hanscom AFB
Massachusetts 01731-5000

PL-TR-91-2240

To be presented at the Eighth International Conference on Interactive Information and Processing Systems for Meteorology, Oceanography, and Hydrology, 6-10 Jan 1992, Atlanta, Georgia Sponsored by the American Meteorology Society

The Remote Atmospheric Processing and Information Display (RAPID) System has been developed at the Geophysics Directorate of Phillips Laboratory to provide an environment for the creation and testing of image processing techniques of remotely sensed data. The first objective of RAPID was to provide nowcasts of cloud and precipitation fields. This is done for cloud fields by tracking and extrapolating contours of infrared bright temperatures from a geostationary satellite. Precipitation fields are forecast by tracking and extrapolating radar reflectivity contours. Currently, there are three techniques in RAPID to extrapolate the future position and shape of contours. The three techniques are the Whole Contour, Segmentation, and Statistical Extrapolation methods. The are all similar in that the contours are represented mathematically, the mathematical features are extrapolated out in time, and forecasted features are used to construct the forecast contour. Tests of the three techniques were conducted using data from the GOES satellite (IR) and the Phillips Laboratory's 10-cm Doppler weather radar. The initial results indicate that, for both satellite and radar data, all three methods do show skill with respect to persistence and produce forecasts that are comparable to each other.

Nowcasting, Precipitation, clouds, radar, satellite

8

Unclassified Unclassified Unclassified SAR

PL-TR-91-2240

NOWCASTING CLOUD AND PRECIPITATION FIELDS USING THE REMOTE ATMOSPHERIC PROCESSING AND INFORMATION DISPLAY (RAPID) SYSTEM

Frank H. Ruggiero and Kenneth F. Heideman

Geophysics Directorate, Phillips Laboratory
Hanscom AFB, Massachusetts

1. INTRODUCTION

In the next few years civilian and military weather forecasters will see a significant increase in the amount of data available for short-term forecast preparation. This increased data includes WSR-88D (NEXRAD) Doppler radars, automated field observing stations, lightning detection networks, and mesoscale numerical models. While the additional data should help, it might be hard for the forecaster to assimilate it all because short-term forecasts, in order to be of any use, must be made quickly. To assist the Air Force weather forecaster make optimal use of this wealth of data the Geophysics Directorate of Phillips Laboratory (formerly the Air Force Geophysics Laboratory) initiated the Advanced Meteorological Processing System (AMPS) project. The objective of AMPS is to integrate current and future sources of weather information and produce products that are directly applicable to forecast problems (Chisholm et al., 1989). Since AMPS products are being designed to operate at base forecast offices, techniques developed need to run in a workstation environment.

A significant portion of the current AMPS effort has been devoted to the nowcasting (0-2 hours) of cloud and precipitation fields. Accurate nowcasts of precipitation and clouds would help promote more efficient air terminal and range operations. In addition, short-term forecasts of heavy precipitation are an important part of flash flood forecasting. Within AMPS this research effort is divided into two parts. One part is the detection and forecasting of the initiation of convective development by the use of a mesoscale 4-D assimilation model (Cotton et al., 1988). The second effort, which will be discussed here, is the objective tracking and forecasting of existing cloud and precipitation areas. This is the initial problem that the Remote Atmospheric Processing and Information Display (RAPID) system was developed to handle. RAPID forecasts the motion and evolution of cloud fields by tracking and forecasting contours of infrared brightness temperatures from geosynchronous satellite data. Precipitation fields are forecast by using radar reflectivity contours. Currently, RAPID has three different forecast methodologies for extrapolating the motion of radar and satellite contours. In this paper we will describe the current implementation of RAPID and provide the results of an evaluation of the forecast techniques.

2. BACKGROUND

The extraction of motion of features of remotely sensed data has been going on for over 20 years. Leese et al. (1971) used a cross-correlation technique on geosynchronous satellite data in order to estimate upper level wind speeds from cloud motion. Muench and Hawkins (1979) applied the idea to the problem of short-term forecasting of cloud areas using Geostationary Operational Environmental Satellite (GOES) visible data. Using radar data, Bellon and Austin (1978) employed the cross-correlation technique in what was probably the first automated precipitation forecasting system. In the Short Term Automated Radar Prediction (SHARP) system the vector that produces the highest cross-correlation is used to uniformly translate the radar image. This type of system is well suited to widespread stratiform precipitation where the precipitation fields tend to move uniformly and there is not much precipitation echo growth, decay or shape evolution. The NEXRAD storm tracking algorithm, developed primarily for severe storms and based on the work of Bjerkaas and Forsyth (1980), has the ability to track and forecast individual storm cells. It objectively tracks a storm cell by a nearest-neighbor technique and forecasts the future centroid position by linear extrapolation. In the United Kingdom, the operational FRONTIERS system (Howes, 1988) tracks features detected by geostationary satellites and a network of radars. Due to the large scale that FRONTIERS operates on, the forecasting of individual features is necessary. This is done by linear

extrapolation of features selected interactively by the forecaster. Andersson and Ivarrson (1991) have developed a probabilistic short-term precipitation forecasting technique that uses 850 mb model output winds to give the current rainfall field a uniform translation.

3. DESCRIPTION OF RAPID

The initial hardware configuration of RAPID has been described by Sadowski et al. (1988). Originally it was planned that the image processing be done on an Adage 3000 image processor. While the Adage is still part of the configuration, all the image processing described here is done on a MicroVAX III GPX workstation. The main reasons for this are the ease of software development on the workstation and the fact that a base weather station will more likely have access to a workstation like the MicroVAX III than to a high powered image processor. The RAPID workstation is part of a VAXcluster of computers in the Air Force Interactive Meteorological System (AIMS) based in the Atmospheric Sciences division of the Geophysics Directorate. Through the cluster RAPID can access real-time satellite data from the Geophysics Directorate GOES ground station. Data can also be acquired via a 9600 bpi land line from the Geophysics Directorate 10 cm wavelength Doppler Weather Radar located 20 miles away in Sudbury, Massachusetts. The Sudbury radar is configured much like the WSR-88D radars. The AIMS cluster currently provides real-time links to the FAA 604 data line and the State University of New York at Albany's Lightning Detection Network. In addition, an Air Force Automated Weather Distribution System (AWDS) terminal that provides conventional observations, model generated analysis and forecast gridded fields is co-located with AIMS.

The RAPID software package (Bianco and Huang, 1990) takes satellite and radar fields and transforms them into Cartesian coordinate planes. The GOES satellite data is converted from its distorted planer coordinate system to a Lambert conformal conic projection. The Lambert projection was chosen because many of the synoptic displays available from AIMS are in that coordinate system. The transformation to Lambert grid is done by determining the latitude and longitude for each grid location in a 256x256 element grid of 8 km resolution. The GOES line and element for that latitude and longitude is found and its value is assigned to the particular pixel on the Lambert grid. This conversion currently takes a long time on the workstation and must be done for every image because of satellite drift. Hopefully, when GOES-NEXT is operational, a more efficient method of using look-up tables can be used since GOES-NEXT will have a more advanced on-board navigation capability. The radar Cartesian grid is actually a composite reflectivity display. To construct the display Cartesian grids for every elevation angle in the radar's volume scan are produced using a bilinear interpolation scheme. Then, for each horizontal pixel location in the composite grid, the highest reflectivity value over that point is assigned to the pixel. For the SHARP system, Bellon and Austin (1978) used 3 km Constant Altitude Planned Position Indicator (CAPPI) displays because of the loss of low elevation features at far range using single low elevation scans. The composite reflectivity product is used here because it uses all the information available in a volume scan. Given that the highest elevation in some of the volume scans received from the Sudbury radar is 4.5°, 3 km CAPPI displays would lead to a substantial data gap around the radar. Using the composite reflectivity display also has the advantage that it is an existing NEXRAD product. Once in a Cartesian grid both the satellite and the radar images are put through one pass of a median box filter to smooth out contour edges and clean up noise. The filtering allows subsequent processing to be faster since very small scale features are eliminated. This does not affect the forecasts since the forecast techniques that we are using do not try to resolve features as small as what we are eliminating.

The satellite brightness temperatures are contoured every 2°K the radar reflectivities are contoured for every 5 dBz. Contours that are less than 16 pixels in circumference are eliminated. Currently, individual contours are tracked manually. The RAPID forecaster can display as many images of a particular sequence as he or she wants (three at a time) and manually select a contour of interest to track, with the aid of a mouse. When a contour is selected for tracking the x and y locations of its boundary are stored and used by the forecast techniques.

Three different forecast techniques have been implemented and are being evaluated on RAPID. The forecast techniques in RAPID are designed to track and forecast the motion of individual contours on an image. In addition, the forecast modules forecast the shape and size evolution of the contours. In general, each technique is similar in that it can be broken down into three basic steps 1) define the contour by mathematical features, 2) extrapolate the mathematical features, and 3) construct the forecast contour from the extrapolated feature values.

3.1 Whole Contour Technique

Detailed descriptions of the Whole Contour Technique have previously been presented by Heideman et al. (1990) and Bianco and Huang (1990). A contour is mathematically described by overlaying it

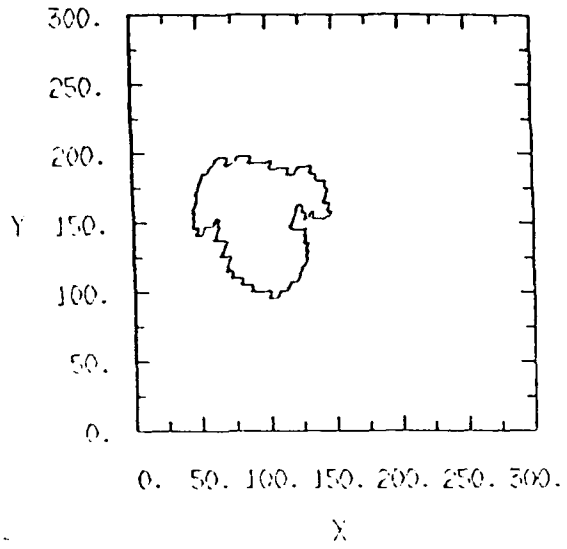

Fig 1. *An example of a GOES IR brightness temperature contour boundary overlaid on a x-y grid plane.*

on a x-y grid as shown in Figure 1. Each location along the contour will then have an x and y location value associated with it. From the location values the individual x and y functions are available as shown in Figure 2. The Fourier phases and amplitudes for each of the functions are calculated. The number of waves used to describe the contour shape is determined by the forecaster. The contour centroid, aspect ratio, and area are also calculated for each contour. Values for several observations of a single contour are obtained and the features are forecast using linear extrapolation. The forecast contour is constructed by taking the extrapolated Fourier phases and amplitudes and using an inverse Fast Fourier transform to determine the x and y contour boundary locations. The forecast shape is then scaled by the extrapolated aspect ratio and area. Finally, the contour is displaced from its original location to its forecast position using the extrapolated centroid position.

3.2 Adaptive Exponential Smoothing Technique

Another way to mathematically describe the shape of a contour is by the length of lines radiating from the contour centroid. The Adaptive Exponential Smoothing (AES) technique of Kavvas (1988) uses the length of 16 lines that extend from the centroid to the contour boundary at fixed equal angles from each other (Figure 3). For each observed contour the length of each line is recorded along with the centroid position. These 17 features are then extrapolated. The extrapolation is done by adaptive exponential smoothing. This is essentially a weighted linear least-squares fitting procedure with an exponentially discounted smoothing coefficient. The value of the smoothing coefficient is determined by the forecaster and can vary between 0 and 1. A low value of the smoothing coefficient makes the extrapolation more responsive to older observations, while a higher value puts more emphasis on newer observations. Because strict linear interpolation is not employed it is hoped that accounting for the growth and decay of precipitation and cloud areas will result in more accurate forecasts. The forecast contour is constructed by plotting the forecast

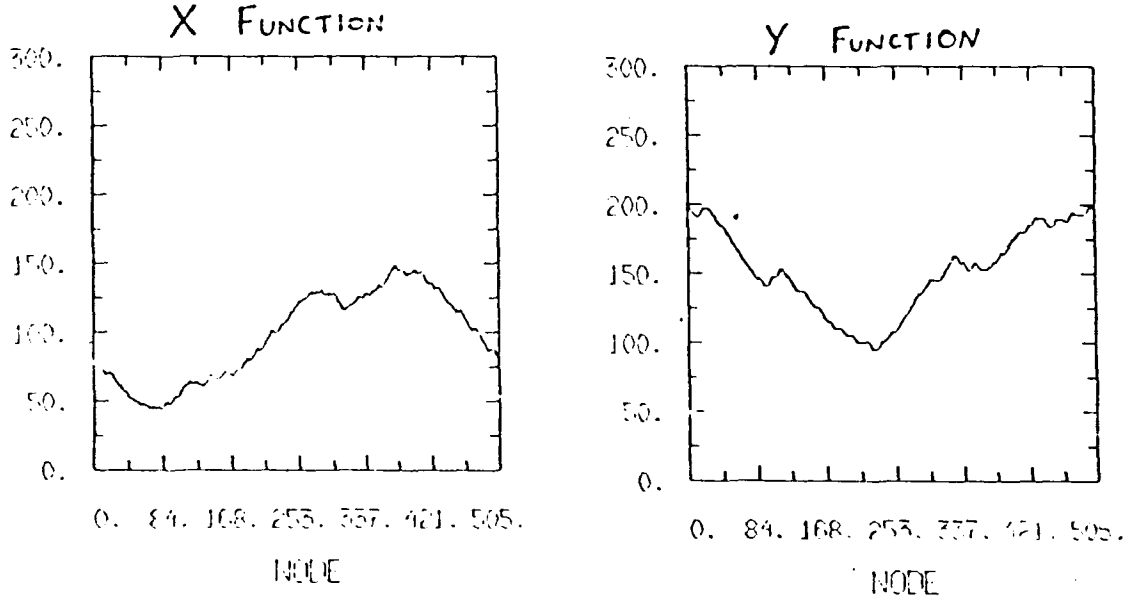

Fig 2. *The functions of x and y for the contour boundary shown in Figure 1.*

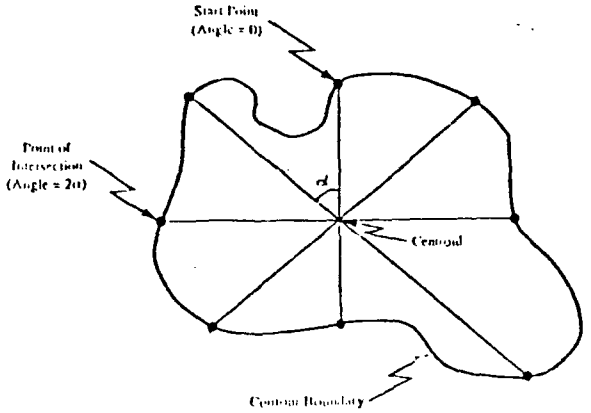

Fig 3. *An example of a contour being described by the Adaptive Exponential Smoothing and Segmentation techniques. The contour is described by the centroid location and the length of lines from the centroid to the contour boundary (After Bianco and Huang, 1990).*

centroid position and laying out the extrapolated line segments from the centroid. The forecast contour boundary is completed by connecting the endpoints of the line segments.

3.3 Segmentation Technique

The Segmentation technique described by Bianco and Huang (1990) essentially uses the same method as the Adaptive Exponential Method to mathematically describe contours and construct forecast contours. The only difference is that the Segmentation method allows the forecaster to select the angle displacement between line segments, which in effect determines how many line segments are used to define the contour. For extrapolation the segmentation method uses a linear least-squares fitting technique.

4. FORECAST EVALUATION

In evaluating the forecast techniques currently available on RAPID there are three main objectives. First, to determine the optimal value or range of values of the selected input parameters for each technique. The second objective is to compare the forecasts of the three techniques generated by RAPID with persistence to see if the techniques show any skill. Our third objective is to compare the techniques with each other to determine if there is one technique that can be the focus of future refinement.

For each technique forecasts were made and verification results processed for various parameter values using different forecast lead times and different numbers of observations for the extrapolation. The range of parameter values tested for the three techniques is given in Table 1. The bounds were chosen based on a preliminary look at a subset of the radar and satellite evaluation results.

To conduct the evaluation, satellite and radar data were acquired to provide a test data set. Satellite data from the Geophysics Directorate GOES ground station were archived on a case by case basis in the spring of 1990. The data ingested into RAPID was 4 km resolution data from the IR 11 μm channel. The field of view was centered over Marseilles, Illinois (42°21' N, 88°41'W) in order to minimize the satellite viewing angle distortion. Eight days of data were archived and 40 cases of contours of IR brightness temperature were selected to be tracked and forecasted. The archives of the Geophysics Directorate's Sudbury radar were searched for cases where the radar was in a continuous NEXRAD-type scanning mode and had trackable reflectivity contours that stayed within the radar viewing domain for at least 40 minutes. Eight days of data produced 17 trackable contours. The relatively small number of trackable contours identified is more a reflection of limitations imposed by our verification scheme than of limited applicability of the techniques.

4.1 Evaluation Methodology

For the purposes of comparing forecasts made by the techniques, each pixel of the domain comprising the radar or satellite image (256x256 pixels) was considered a categorical forecast and observation point. By comparing the position of forecast contours with the verification imagery valid for the same time each pixel could be assigned to one element of a two by two contingency table (see Figure 4). Note that while correct forecasts of non-events (box d in Figure

Technique	Input Parameter	Bounds
Whole Contour	Maximum Wave Number	1-5
Adaptive Exponential Smoothing	Smoothing Coefficient	.2 - .4 (by 0.05)
Segmentation	Displacement Angle	5° - 20° (by 5°)

Table 1. The user supplied parameters for each technique and the bounds on the values used in the evaluation.

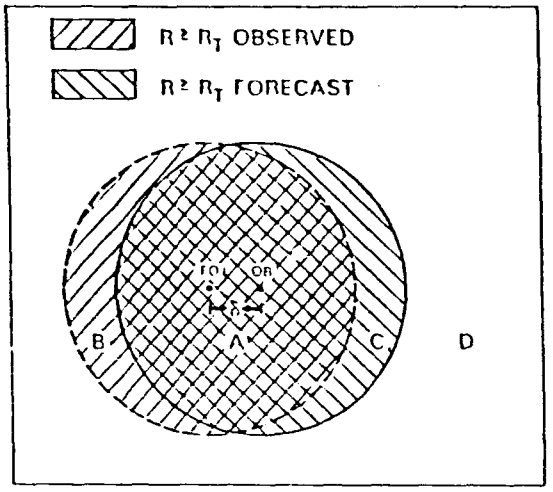

OBSERVED \ FORECAST	$\geq R_T$	$< R_T$
$\geq R_T$	A	B
$< R_T$	C	D

FO FORECAST AREA CENTROID
OB OBSERVED AREA CENTROID
δ DISTANCE BETWEEN CENTROIDS
R_T THRESHOLD RADAR REFLECTIVITY

Fig 4. *Schematic of hypothetical forecast and observed radar reflectivity contours and associated contingency table.*

4) are important components of many skill scores (Mason, 1982 and Schaefer, 1990), including them in our pixel by pixel evaluation resulted in artificially inflated scores. The scores used in this evaluation are thus restricted to use of the first three elements of the contingency table.

Bias is the ratio of the number of pixels forecasted to contain radar reflectivity values above a specified threshold, to the number observed (bias is greater than one for overforecasts and less then one for underforecasts),

$$bias = (a+c)/(a+b). \quad (1)$$

False alarm ratio (FAR) ranges from 1 (worst) to 0 best,

$$FAR = c/(c+a). \quad (2)$$

Probability of detection (POD) ranges from 0 (worst) to 1 (best),

$$POD = a/(a+b). \quad (3)$$

The Critical Success Index (CSI) (Donaldson et al, 1975) combines elements of the POD and FAR and ranges from 0 (worst) to 1 (best),

$$CSI = a/(a+b+c). \quad (4)$$

Care must be used when interpreting CSI scores. Comparing CSI scores for forecasts on different data sets is not valid. Therefore, scores from the radar and satellite cases should not be compared with each other.

WHOLE CONTOUR

# OF WAVES	RADAR	SATELLITE
1	0.33	0.44
2	0.34	0.44
3	0.32	0.43
4	0.32	0.43
5	0.31	0.43

Table 2. Average Critical Success Index scores for forecasts of the Whole Contour Technique using varying numbers of waves to describe the contour.

Persistence forecasts were also generated and evaluated using the procedure outlined above. For our purpose persistence is defined as the most recent observed contour. For example, if you have observed contours at time 1,2, and 3 and you want to make a forecast for time 4, the persistence forecast is simply the observed contour at time 3.

4.2 Evaluation Results

First, the forecasts were run using each technique on all satellite and radar data while varying the technique dependent input parameters values. The results are in Tables 2 - 4. Clearly, while there is some variation in the forecast accuracy as measured by CSI, the differences are small enough that they cannot be considered significant.

The parameter values associated with the highest CSI scores in the radar and satellite data sets for each technique were used to compare the techniques. The results of the comparisons are shown in Figure 5 for the radar data. While all three of the techniques seem to be roughly equivalent in score it should be noted that all the techniques for both radar and satellite data produce forecasts that are substantially better than persistence.

FAR and POD scores for the Segmentation method on radar data (Fig. 6) show that the forecast technique has a high probability of detection of over 70%

ADAPTIVE EXPONENTIAL SMOOTHING

SMOOTHING COEFFICIENT	RADAR	SATELLITE
0.20	0.24	0.34
0.25	0.28	0.37
0.30	0.30	0.39
0.35	0.30	0.39
0.40	0.29	0.39

Table 3. Average Critical Success Index scores for forecasts of the Adaptive Exponential Smoothing Technique using different smoothing coefficients.

SEGMENTATION

DISPLACEMENT ANGLE	RADAR	SATELLITE
5°	0.33	0.44
10°	0.35	0.44
15°	0.35	0.37
20°	0.36	0.43

Table 4. Average Critical Success Index scores for forecasts of the Segmentation Technique using different values of the displacement angle.

for the first 30 minutes. However, in that same time period the FAR rises from under 40% at 12 minutes to near 60% at 30 minutes. The Adaptive Exponential Smoothing and Whole Contour Techniques exhibited similar tendencies for the radar cases. The high values of the FAR indicate a systematic over-forecasting of the contour size. This is also reflected in the bias scores for the radar forecasts which average over 1 for each of the techniques.

Figure 7 shows the comparison of the forecast techniques for satellite data. The techniques are approximately equal in forecast accuracy for the first two hours, after which the Adaptive Exponential Smoothing technique starts to perform worse than the others. The differences between the forecast techniques and persistence is smaller than compared with the radar data set. However, the largest difference between the techniques and persistence in the satellite data set occurs in the important 1-2 hour time frame. Figure 8 shows the POD and FAR scores for the Segmentation technique on satellite data. The POD scores for the early forecast times are lower than they were for the radar data but remain relatively level. The FAR increases as the forecast lead times become greater,

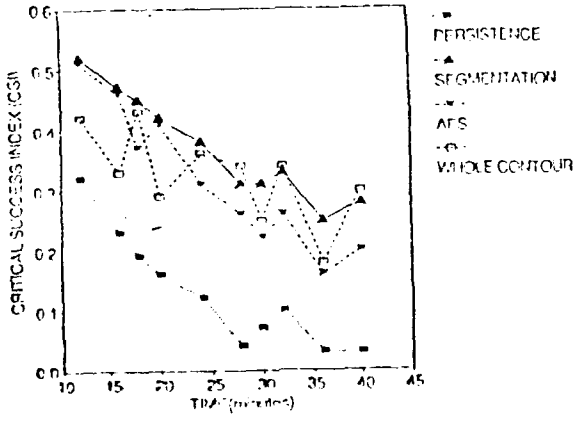

Fig 5. Plot of CSI scores for each forecast technique and persistence as a function of forecast lead time for radar cases.

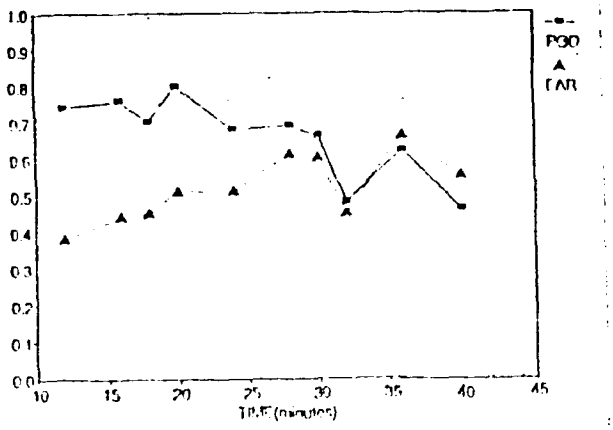

Fig 6. Plot of Probability of Detection (POD) and False Alarm Rate (FAR) as a function of forecast lead time for the Segmentation technique using radar data.

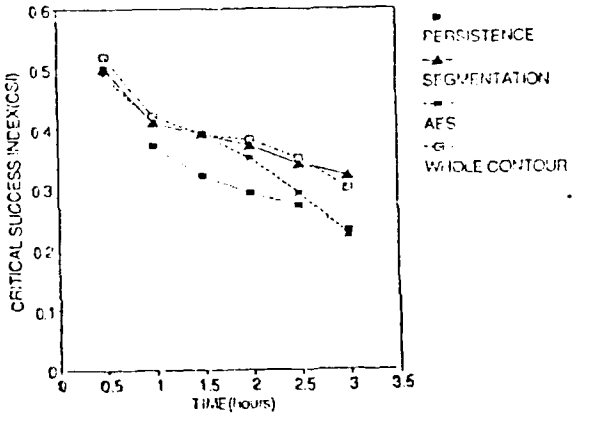

Fig 7. Plot of CSI scores for each forecast technique and persistence as a function of forecast lead time for satellite cases.

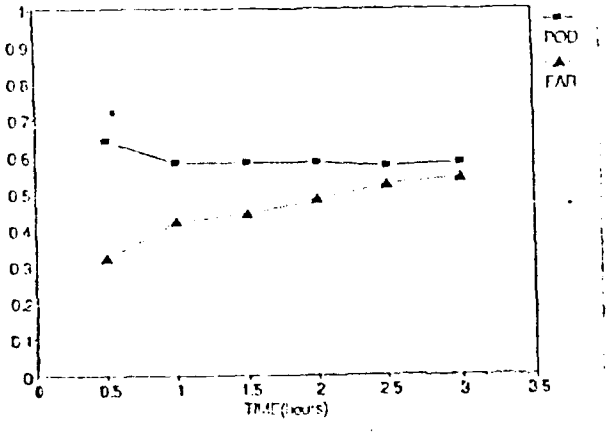

Fig 8. Plot of Probability of Detection (POD) and False Alarm Rate (FAR) as a function of forecast lead time for the Segmentation technique using satellite data.

thus reducing the CSI scores. As with the radar data the increasing FAR scores are a result of systematic over-forecasting of the contour area as indicated by bias scores over 1.

5. SUMMARY AND CONCLUSIONS

A workstation-based system for making short-term forecasts of cloud and precipitation fields using remotely sensed data has been described. Three different techniques for forecasting the fields have been evaluated. Overall the forecast techniques produced forecasts that were generally superior to persistence. The techniques as presently configured can be applied to radar data in situations where there is a need for a high probability of detection and a relatively high false alarm rate can be tolerated. The evaluation results do not reveal which parameter values provide the best forecasts nor do they reveal which technique can be considered the best. On an individual forecast basis there are situations where one of the techniques shows much better results than the others. It may be that single no method performs the best under all conditions.

6. FUTURE PLANS

Evaluation of the short-term forecasting techniques described here will continue on RAPID using an enlarged satellite data base to include data from all seasons. With a larger data base we might be able to stratify the results and determine under what conditions a particular technique and or parameter value gives the best results. The ultimate goal is to come up with an algorithm and product that can be implemented into AWDS when it begins to receive Geostationary Satellite data. Further evaluation and implementation of one of the forecast techniques into NEXRAD will be handled by the Ground Based Remote Sensing branch of the Geophysics Directorate.

A new effort involving RAPID will be to incorporate data from polar orbiting satellites, the lightning detection networks, model fields generated by locally run mesoscale models, and global circulation models available from AWDS to help detect areas of precipitation where there is no ground-based radar data.

7. Acknowledgements

The authors wish to thank the system managers of the AIMS VAXcluster, Charles Ivaldi and Joseph Doherty, for their help in developing some of the necessary software for this effort. We would also like to thank Tim Hiett and the members of the Ground Based Remote Sensing Branch for their help in collecting the radar data used in this study.

REFERENCES

Andersson, T. and K. Ivarsson, 1991: A Model for Probability Nowcasts of Accumulated Precipitation using Radar. J. Appl. Meteor., 30, 135-141.

Bellon, A. and G.L. Austin, 1978: The Evaluation of Two Years of Real-Time Operational of a Short-Term Precipitation Forecasting Procedure (SHARP). J. Appl. Meteor., 17, 1778-1787.

Bianco, A. and H. Huang, 1990: Satellite and Radar Forecast Techniques for Short-Term Prediction of Storm Motion on the Remote Atmospheric Processing and Display (RAPID) System. Geophysics Laboratory Technical Report GL-TR-90-0179 43pp.

Bjerkaas, C.L. and D.E. Forsyth, 1980: Operational Test of a Three-Dimensional Echo Tracking Program. Preprints, 19th Conf. Radar Meteorology, Miami Beach, Amer. Meteor. Soc., 244-247.

Chisholm, D.A., A.R. Bohne, and R.M. Dyer, 1989: The Development of Numerically-Based and Expert System Approaches for Airfield Nowcasting/Very Short Range Forecasting. 3rd Int. Conf. Aviation Weather System, Anaheim, Amer. Meteor. Soc., 433-436.

Cotton, W.R., R. McAnelly, C. Tremback, and R. Walko, 1988: A Dynamic Model for Forecasting New Cloud Development. Air Force Geophysics Laboratory Technical Report, AFGL-TP-89-0011, 83pp ADA213939.

Donaldson, R.J., Jr., R.M. Dyer, and M.J. Kraus, 1975: An Objective Evaluator of Techniques for Predicting Severe Weather Events. 9th Conf. Severe Local Storms, Norman, pp 321-326.

Heideman, K.F., H. Huang, and F.H. Ruggiero, 1990: Evaluation of a Nowcasting Technique based on GOES IR Satellite Imagery. 5th Conf. Satellite Meteor. and Ocean., London, pp366-371.

Howes, S., 1988: Use of Satellite and Radar Images in Operational Precipitation Nowcasting. J. British Interplanetary Society, 41, 455-460.

Kavvas, M.L. and Z. Chen, 1989: The Radar-Based Short-Term Prediction of the time-space evolution of rain fields. Geophysics Laboratory Technical Report, GL-TR-89-0103, ADA213802.

Leese, J.L., C.S. Novak, and B.B. Clark, 1971: An Automated Technique for Obtaining Cloud Motion from Geosynchronous Satellite Data Using Cross Correlation. J. Appl. Meteor., 10, 118-132.

Mason, I., 1982: A Model for Assessment of Weather Forecasts. Australian Meteorol. Magazine, 30, 291-304.

Muench, H.S. and R.S. Hawkins, 1979: Short-Range Forecasting Through Extrapolation of Satellite Imagery Patterns Part 1: Motion Vector Techniques. AFGL Technical Report AFGL-TR-79-0096, 21pp ADA073308.

Sadowski P.A., A.R. Bohne, and F.I. Harris, 1988: AFGL Remote Atmospheric Processing and Interactive Display (RAPID) System. Preprints, Fourth Int. Conf. on Interactive Information and Processing Systems for Meteorology, Oceanography, and Hydrology, Anaheim, California, Amer. Meteor. Soc., 233-240.

Schaefer, J.T., 1990: The Critical Success Index as an Indicator of Warning Skill. Wea. Forecasting, 5, 550-575.